

1 **Relative tectonic activity classification in Kermanshah**
2 **area, west Iran**

3 **M. ARIAN¹ and Z. ARAM²**

4 [1]{*Department of Geology, College of Basic Sciences, Tehran Science and Research*
5 *Branch, Islamic Azad University, Tehran, Iran*}

6 [2]{*Department of Geology, Kermanshah Branch, Islamic Azad University,*
7 *Kermanshah, Iran*}

8 Correspondence to: M. ARIAN (mehranarian@yahoo.com)

9

10 **Abstract**

11 The High Zagros region because of closing to subduction zone and the collision of the
12 Arabian and Eurasian plates is imposed under the most tectonic variations. In this
13 research, Gharasu river basin that it has located in Kermanshah area was selected as the
14 study area and 6 geomorphic indices were calculated and the results of each ones were
15 divided in 3 classes. Then, using the indices, relative tectonic activity was calculated
16 and the values were classified and analyzed in 4 groups. Regions were identified as
17 very high, high, moderate and low. In analyzing the results and combining them with
18 field observation and regional geology the results are often associated and justified with
19 field evidences. The highest value is located on Dokeral anticline in crush zone in
20 Zagros Most of the areas with high and moderate values of lat are located on crush zone
21 in Zagros too. Crushing of this zone is because of main faults mechanism of Zagros
22 region. The result of this paper confirms previous researches in this region. At the end
23 of the eastern part of the study area, the value of Iat is high that could be the result of
24 Sarab and Koh-e Sefid faults mechanism.

25

26 **Keywords:** Morphometry, Tectonic, Quaternary, Zagros, Iran,

27 **1. Introduction**

28 The study area is Gharasu river basin, which is at west of Iran. The river is located in
29 the Zagros fold-thrust belt in Kermanshah Block (Fig.1). The aim of selection the basin,
30 as study area is to calculate different geomorphic indices to assessment active tectonics
31 of the area. North-eastern area consists of thin imbricate Fan (thrust sequence) that
32 cause the creation of fault breccias, shear zones, general crushing of formations with
33 development of linear joint system ,suddenly cutting of layers and changed of their age
34 and lithology in nearly. In the area we can see a lot of tectonic windows (Karimi, 1999).

35 Since the rivers were sensitive to the recent tectonic activities of there and show the
36 rapid reaction, Gharasu River and other secondary rivers are selected for calculation of
37 the indices. Geomorphologic studies of active tectonic in the late Pleistocene and
38 Holocene are important to evaluate earthquake hazard in tectonically active areas such
39 as Zagros (Keller and Pinter, 2002).

40 In this study Gharasu basin is divided to 89 subbasin and if possible, each of below
41 indices are calculated: stream –gradient index(SI), drainage basin asymmetry (*Af*),
42 hypsometric integral(Hi), valley floor width-valley height ratio(*Vf*), drainage basin
43 shape(Bs), and mountain-front sinuosity(*J*).We use geomorphic indices of active
44 tectonics, known to be useful in active tectonic studies (Bull and McFaden,1977; Azor
45 et al., 2002; Molin et al., 2004; Silva et al., 2003; Keller and Pinter, 2002) methodology
46 has been previously tested as a valuable tool in different tectonically active areas, we
47 can point to SW USA (Rockwell et al,1985), the Pacific coast of Costa Rica ,(Wells et
48 al., 1988), the Mediterranean cost of Spain(Silva,1994), the south-western Sierra
49 Nevada of Spain (El Hamdouni et al., 2007), and the Sarvestan area in central Zagros of
50 Iran (Dehbozorgi et al., 2010), and these studies are useful. Also the results must be
51 combined to geology studies of the region and field observations in order to obtain
52 desire result.

53 **2. Regional and geological setting of the study area**

54 The area is located between latitudes 34 to 35 northern degree and longitudes 46.30 to
55 47.30 western degree. The study area (3470 km²) is located along part of the Zagros
56 fold-thrust belt ,with length 1500 meter ,is extended from Taurus mountain at
57 southeastern Turkey to Minab fault at east of Strait of Hormoz (Mirzaei et al., 1998).

58 The study area according to division (Braud 1979) contains some part of autochthon
59 Zagros and allochthon Zagros and thin imbricate Fan (thrust sequence) (Fig. 2). Thrust
60 dips in the area are less than 45 degree, but sometimes reaches to 70 degree and formed
61 reverse faults (Karimi,1999).the accomplished studies on area joints shows that the
62 largest direction of main stress axis is form north ,north-east to south ,south-west
63 (Nazari, 1998).

64 Since the area is influenced by Arabian plate pressure and thrust of Central Iran occur
65 offer the omission of Neotethys ocean, on Arabian plate, some of the faults are of thrust
66 kind and have the northwest-southeast trending and the thrust vergency is southwest.

67 **3. Materials and methods**

68 To study the indices there is a formula which we turn to description each of indices;

69 **3.1 The stream –gradient index (SL):**

70 Rivers flowing over rocks and soils of various strengths tend to reach an equilibrium
71 with specific longitudinal profiles and hydraulic geometrics (Hack, 1973; Bull,
72 2007).Hack (1957, 1973, 1982) defined the stream-gradient index (SL) to discuss
73 influences of environmental variables on longitudinal stream profiles, and to test
74 whether streams has reached an equilibrium. The calculation formula is in this manner:
75 $SL = (\Delta H / \Delta L) L$ (1)

76 Where $(\Delta H / \Delta L)$ is local slope of the channel segment that locates between two
77 contours and L is the length channel from the divide to the midpoint of the channel
78 reaches for which the index is calculated.

79 **3.2 Asymmetry factor (Af):**

80 This index is related to two tectonic and none tectonic factors. None tectonic factor may
81 relate to lithology and rock fabrics. It is away to evaluate the existence of tectonic
82 tilting at the scale of a drainage basin. The method maybe applied over a relatively large
83 area (Hare and Gardner, 1985; Keller and Pinter, 2002). The index is defined as
84 follows:

$$85 Af = (A_r / A_t) 100 \quad (2)$$

86 Where A_r is the right side area of the basin of the master stream (looking downstream)
87 and A_t is total area of the basin that can be measured by GIS software

88 **3.3 Hypsometric integral index (Hi):**

89 The hypsometric integral (H_i) describes the relative distribution of elevation in a given
90 area of a landscape particularly a drainage basin (Strahler, 1952). The index is defined
91 as the relative area below the hypsometric curve and it is an important indicator for
92 topographic maturity.

93

94 **3.4 Valley floor width-valley height ratio (Vf):**

95 Another index sensitive to tectonic uplift is the valley floor width to valley height ratio
96 (V_f). This index can be separated v-shaped valleys with small amounts from u-shaped
97 valleys with greater amounts. The calculation formula is in this manner:

$$98 \quad V_f = 2 V_{fw} / (A_{ld} + A_{rd} - 2A_{sc}) \quad (3)$$

99 Where V_{fw} is the width of the valley floor, and A_{ld} , A_{rd} and A_{sc} are the altitudes of
100 the left and right divides (looking downstream) and the stream channel, respectively
101 (Bull, 2007). Bull and McFadden (1977) found significant differences in V_f between
102 tectonically active and inactive mountain fronts, because a valley floor is narrowed due
103 to rapid stream down cutting.

104 **3.5 Basin shape index (Bs):**

105 Relatively young drainage basins in active tectonic areas tend to be elongated in shape
106 normal to the topographic slope of a mountain.. The elongated shape tends to evolve to
107 a more circular shape (Bull and McFadden, 1977). Horizontal projection of basin shape
108 may be described by the basin shape index or the elongation ratio, B_s (Cannon, 1976;
109 Ramirez-Herrera, 1998). The calculation formula is: $B_s = B_l / B_w$ Where B_l is the length
110 of the basin measured from the headwater to the mount, and B_w is basin width in
111 widest point of the basin.

112 **3.6 Mountain-front sinuosity index (J):**

113 This index represents a balance between stream erosion processes tending to cut some
114 parts of a mountain front and active vertical tectonics that tend to produce straight
115 mountain fronts (Bull and McFadden, 1977; Keller, 1986). Index of mountain front
116 sinuosity (Bull and McFadden, 1977) and (Bull, 2007) is defined by:

$$117 J=L_j / L_s \text{ (4)}$$

118 Where L_j is the planimetric length of the mountain along the mountain-piedmont
119 junction, and L_s is the straight –line length of the front.

120 **4. The calculation and analyzing of indices in the study area**

121 It is necessary to have some primary maps to calculate the indices, which the most
122 important of them are: Digital Elevation Model (DEM) and the drainage network and
123 subbasins map of the Gharasu river basin that they have been extracted from DEM.
124 DEM(**ISRTM**) extracted from a digitized topographic map(**1:30000**)

125 **4.1 Stream – gradient index (SL):**

126 To calculate the amount of $(\Delta H/\Delta L)$ and L , we need the contour and drainage network
127 map. The contours are gained from DEM. In this study contours distances are selected
128 10 meters. This index is calculated along the master river for each subbasin (fig. 3) and
129 then computed SL average for each one. Amount of SL not calculated for 2 subbasin
130 (49 and 57) because the values of contours which cut the master river are not enough.

131 In table 1, subbasin84 is brought up as example. The SL index can be used to evaluate
132 relative tectonic activity (Keller and Pinter, 2002). An area on soft rocks with high SL
133 values can be indicates to active tectonics.

134 SL value is classified into 3 categories, which are: class 1($SL>500$), class2
135 ($300<SL<500$), and class3 ($SL<300$), (El Hamdouni et al., 2007). The minimum value
136 of SL is 1.33, in subbasin2, and the maximum value is 7893.97 in subbasin 88. After
137 averaging each subbasin, the maximum value is obtained to subbasin 88(16669) and
138 two subbasin 49 and 57 are not value (Table 1).

139 The mentioned index changes in stones with various resistances. The high resistances of
140 rocks cause to increase amount of the index. Anomaly in SL can show the tectonic
141 activity. So in order to analysis of this index, the map of stones resistance is prepared

142 (fig.4). In this map, the stones with very low resistance (young alluvial deposits), low
143 resistance (older alluvial fan deposits), moderate resistance (shale and silt), high
144 resistance (limestone, tuff, conglomerate, sandstone) and very high resistance
145 (monzodiorite, monzogabbro and quartesite) are specified(Memarian, 2001).

146 By studying SL values we can find that in northern part of the area, in spite of the
147 existence of very high resistance stone, SL value decrease (Fig.3). The reason is intense
148 breakage of sediments and volcanic rocks, which thrust on others by upthrusting . We
149 see in SL map(fig.9) that most of the subbasin with high and moderate SL values are
150 located in the middle part of the study area which has the same trending with strike of
151 main valleys and faults (Northwestern- Southeastern).Major exposed rocks in above
152 area are crushed limestone. In southern part of the area the tectonic activity is often low
153 which its main reasons is going out from the active fault and low resistance of rock and
154 young alluvial deposits. Some of the longitudinal river profiles and the measured SL
155 index are shown on fig.5.

156 **4.2 Asymmetric factor (Af):**

157 To calculate this index in the area A_t and A_r are obtained by using of the subbasins and
158 the master river maps. A_f is close to 50 if there is no or little tilting perpendicular to the
159 direction of the master stream. A_f is significantly greater or smaller than 50 under the
160 effects of active tectonics or strong lithologic control. The values of this index is
161 divided to three categories.1:($A_f < 35$ or $A_f > 63$) 2:($57 < A_f < 65$) or ($35 < A_f < 43$) and
162 3:($43 < A_f < 57$)(El Hamdouni et al.,2007) (Table 1).

163 Among the obtained values, the minimum value belongs to subbasin 65 with 13.89
164 percent and the maximum value belongs to subbasin 6 with 91.81 percent. About this
165 index, we often see all categories are scatter. But class 3 is seen in the valleys and the
166 subbasins with low dip and class 1 in southwestern margin in the study area.

167 **4.3 Hypsometric integral (Hi):**

168 H_{max} , H_{min} and H_{ave} are calculated on DEM here. This index is calculated to all
169 subbasins in the area and the minimum value is 0, 07 for subbasin 56 and maximum
170 value is 0.53 for subbasin 63(Table1). We can also obtain the amount of hypsometric
171 integral from the area under the curve (fig. 6).

172 The hypsometric integral reveals the maturity stages of topography and can be
173 indirectly an indicator of active tectonics.

174 In general, high values of the hypsometric integral are convex, and these values are
175 generally >0.5 . Intermediate values tend to be more concave-convex or straight, and
176 generally have values between 0.4 and 0.5. Finally, lower values (<0.4) tend to have
177 concave shapes (El Hamdouni et al., 2007).

178 On interpretation of the hypsometric index map the interesting point is that the high to
179 moderate values in middle part of the study area approximately are according to SL
180 anomalies. The high and moderate values in this part have NE-SW trending (according
181 to trending of the area fault). Of course, there are other subbasins with high and
182 moderate value after the mentioned area often shows the increase in subbasins which is
183 located near of Gharasu River in the south-eastern corner of the study area.

184 **4.4 Ratio of valley floor width to valley height (V_f):**

185 Bull and McFadden (1977) found significant differences in V_f between tectonically
186 active and inactive mountain fronts (fig. 7), because a valley floor is narrowed due to
187 rapid stream down cutting.

188 Valleys upstream from the mountain front tend to be narrow (Ramirez-Herrera, 1998),
189 and V_f is usually computed at a given distance upstream from the mountain front (Silva
190 et al., 2003). We set a distance to 2 km, and within the mountain range. V_f was
191 calculated for the main transverse valleys of the study area using cross-section drawn
192 from the DEM and topographic map (Fig. 8).

193 V_{fw} value is obtained by measuring the length of a line which cuts the river and limits
194 to two side of a contour that the river crosses among it. Values of A_{ld} , A_{rd} , and A_{sc} are
195 measured by using the drawn profile. Since finding place of V_f is independent from the
196 subbasins, so it is possible that some of them have no V_f and some others have various
197 V_f values (Table 1). V_f values are divided into 3 classes: 1 ($V_f < 0.3$), 2 ($0.3 < V_f < 1$),
198 and 3 ($V_f > 1$) (El Hamdouni, 2007) (Fig. 9).

199 Some subbasins, because of absence the suitable valley, have no value and others have
200 values from zero for subbasin 1, to 19.44 for subbasin 66. Most of the valleys are in
201 class 3 and show the U shape of the valleys. But the moderate to high values often locate

202 at northern part of the study area. The interesting point is in middle part of the area V_f
203 index, at northwestern-southeastern direction like other indices as SL and Hi, shows
204 moderate to high classes, which is according to main faults of Zagros.

205 **4.5 Basin shape index (Bs):**

206 To calculate this index in the area Bl and Bw are obtained by using of the subbasins and
207 the master river maps and the values are divided in 3 classes.1:(Bs>4) 2:(3<Bs<4)
208 3:(Bs<3) (El Hamdouni et al.,2007) (Fig. 9;Table 1). The minimum value belongs to
209 subbasin 56 with 0.7 and the maximum value belongs to subbasin 31 with 6.37. The
210 other subbasins have a value between these two values.

211 Bs values show a few activities in most parts of the study area, but classes 2 and 3 are
212 often, scatter in southwestern margin and the middle part of the study area.

213 **4.6 Mountain-front sinuosity index (J):**

214 The Mountain fronts of the study area by helping of faults and folds site is drawn. J is
215 commonly less than 3, and approaches 1 where steep mountains rise rapidly along a
216 fault or fold (Bull, 2007). Therefore, this index can play the important role in tectonic
217 activity. By considerate that mountain fronts sites are independent of subbasins place,
218 so it is possible some of them have various fronts and the others have no mountain
219 fronts (Table 1).

220 Values of J are readily calculated from topographic maps or aerial photography. The
221 values of J calculated for 36 mountain fronts (Fig. 7).J values are divided to 3 classes: 1
222 ($J<1.1$), 2($1.1<J<1.5$), and 3($J>1.5$) (El Hamdouni, 2007).

223 In the study area most of the obtained values are between 1.1 to 1.5 (class 2) and the
224 parts which are in class 3 often locate in northern part of the area. It needs to be
225 mentioned that class 1 is not exist in the study area (Fig. 9).

226 **5. Results and discussion**

227 The average of the six measured geomorphic indices (V_f , J, Bs, Af, Hi, and SL) was
228 used to evaluate the distribution of relative tectonic activity. Each of the indices, were
229 divided to 3 classes. With averaging of these six indices we obtain one index that is
230 known relative active tectonic (Iat) (El Hamdouni et al., 2007). The values of the index

231 were divided into four classes to define the degree of active tectonics: 1-very high
232 ($1 < I_{at} < 1.5$), 2-high ($1.5 < I_{at} < 2$), 3-moderate ($2 < I_{at} < 2.5$), 4-low ($2.5 < I_{at}$) (El Hamdouni
233 et al., 2007)

234 The distribution of the four classes is shown in Fig. 10. In this map the high and
235 moderate values of I_{at} in middle part of the area is obvious, and the subbasin 1, 2, and
236 6(at the end of southwestern of the area) have high to moderate values of I_{at} too. **Table**
237 **2** shows the result of the classification for each subbasin. **Also, base on Arian and**
238 **Hashemi (2008), this area is a high seismic risk zone with follow seismicity parameters:**
239 **$a = 3.79$, $b = 0.50$, $\beta = 1.72$ and Λ for $M=4$ is 1.47.**

240

241 **6. Field evidence of active tectonics**

242 In the study area from south to north we have 3 subdivided: 1- autochthon Zagros 2-
243 radiolaritic overthrust nappes, Bisotun limestone and Ophiolite 3- Thin imbricates Fan
244 (thrust sequence) (Braud, 1979). At north parts of the area complex of flysch
245 (Cretaceous – Paleocene) and Ophiolite Assemblage (like disturbed basic layer) are
246 appeared.

247 In Neogene, a basic magma intruded along Morvaride fault (Fig. 11).and formed a
248 broad gabbro-diorite massive body in the north Kamyaran. The function of tectonic
249 phases cause to existence regional metamorphism like green schist facies in flysch
250 stones (Cretaceous – Paleocene).The traces of this metamorphism cause the
251 appearance of serpentine in the area (Sadeghian and Delavar, 2007).

252 At southern part of the area, the thrust fault of listric extensional kind are seen, which
253 their strike are from north-northern west -south- southern east (Karimi, 1999). It seems
254 that the activity of these faults cause to increase the relative tectonic activity to class 3.

255 The limestone of Bisotun and radiolarite of Kermanshah which development in center of
256 the study area have separated from autochthon Zagros by Koh-e Sefid fault. Bisotun
257 limestone is a very thick and main stony unit which contain from upper Triassic to
258 upper cretaceous (Braud, 1979). Bisotun limestone has intense folds (Fig. 12) and faults
259 in the area which cause to make the important anticlines such as Dokral, Naraman,
260 Chalabad, and Shahoo in its direction and class 1, 2, and 3 of I_{at} index which have the
261 same direction to Bisotun limestone are seen in the area.

262 The south western border Kermanshah radiolarite is bounded to Koh-e Sefid fault. (Fig.
263 13).This fault has thrust Kermanshah radiolarites on Amiran flyschs.

264 The thickness of fault breccias in this place reaches to 100 meters. The mentioned
265 breccias are made of radiolarite, limestone, and sandstone elements. The activity of
266 Koh-e Sefid and Sarab faults can be a reason for increasing the relative tectonic activity
267 at the end of the study area.

268 Koh-e Sefid anticline (Fig. 7) is located between Gharasu and Mereg rivers. Although
269 Mereg source is located in 15 km south of Gharasu, but to reach to Gharasu, this river
270 must travel almost 140 km toward northwest trending to join to Gharasu in Doab
271 region.

272 **7. Conclusion**

273 It seems that the calculated geomorphic indices by using of GIS are suitable to
274 assessment of tectonic activity of the study area. The geomorphic indices such as:
275 stream –gradient index (SI), drainage basin asymmetry (Af), hypsometric integral (Hi),
276 valley floor width-valley height ratio (Vf), drainage basin shape (Bs), and mountain-
277 front sinuosity (J), are calculated in Gharasu basin. So, firstly the area was divided to 89
278 subbasins and indices were calculated to each of them, then each of the indices divided
279 to 3 classes. Then, 6 measured indexes for each subbasin were compounded and a unit
280 index obtained as relative tectonic activity (Iat). This index is divided to 4 classes of
281 tectonic activity: very high, high, moderate, and low. The area and occupation
282 percentage each class of indices is calculated. As seen most of the high percentage and
283 areas locate in class 3 that show the low tectonic activity (Table 3).

284 Class 1(Iat) have an area about 28.94 km² (0.53 %), Class 2(Iat) with an area about
285 173.96 km² (3.18 %), Class 3(Iat) with an area about 1162.97 km² (21.26 %), Class
286 4(Iat) with an area about 4104.98 km² (75.03%) are of total area. Class 1 locates around
287 Dokeral anticline, class 2 locates on northeastern flank of Nesar and Naraman
288 Mountain, class 3 is scattered at western border of the study area and a part of it has a
289 same trending with Bisotun limestone in middle part of the study area.

290 The other parts of the area have class 4 of Iat. Subbasin 68 is a single subbasin with very
291 high value of Iat. It is located on Dokeral anticline in a crush zone in Zagros

292 Most of the area with high and moderate value of lat have located on crush zone in
293 Zagros, too. Crushing of this zone is because of main faults mechanism of Zagros
294 region. Since that this faults have NE-SW direction, the area with high and moderate
295 value have tend to development of this trending. The results of this paper confirm
296 previous researches in this region. At the end of the eastern part of the study area, the
297 value of Iat is high that could be the result of Sarab and Koh-e Sefid faults mechanism.
298

299 **8. ACKNOWLEDGEMENT**

300 This work is funded by the Department of geology, Islamic Azad University, Science
301 and Research branch, Tehran, Iran. Also, special thanks to Vice-President for Research
302 in Science and Research branch, Tehran.

303

304 **9. References**

305 [Arian, M., and Hashemi, S. A., 2008. Seismotectonic Zoning in the Zagros. Journal of](#)
306 [Sciences, 18, 69, 63-74.](#)

307 Braud, J., 1979. Geological map of Kermanshah area, scale 1:250000 Geologic Survey
308 of Iran.

309 Bull, W.B. & McFadden, L.D., 1977. Tectonic geomorphology north and south of the
310 Garlock fault, California. In: Doehring D.O. (Ed). Geomorphology in Arid Regions.
311 Proceedings of the Eighth Annual Geomorphology Symposium. State University of
312 New York, Binghamton. 115-138.

313 Bull, W.B., 2007. Tectonic geomorphology of mountains: a new approach to
314 paleoseismology. Blackwell, Malden.

315 Cannon, P.J., 1976. Generation of explicit parameters for a quantitative geomorphic
316 study of Mill Creek drainage basin. Oklahoma Geology Notes 1, 3-16.

317 Dehbozorgi, M., Pourkermani, M., Arian, M., Matkan, A.A., [Motamedi, H.](#) &
318 [Hosseiniasl, A.](#), 2010. Quantitative analysis of relative tectonic activity in the
319 Sarvestan area, central Zagros, Iran. Geomorphology, 121, 329-341.

- 320 El Hamdouni R., Irigaray C., Fernandez T., Chacon J. & Keller EA., 2007.
321 Assessment of relative active tectonics, southwest border of Sierra Nevada (southern
322 Spain). *Geomorphology* 96, 150-173.
- 323 Hack J.T., 1957. Studies of longitudinal stream-profiles in Virginia and Maryland: U.S.
324 Geological Survey Professional Paper 294B, 45-97.
- 325 Hack J.T., 1973. Stream-profiles analysis and stream-gradient index, *Journal of*
326 *Research of the U.S. Geological Survey*, 1, 421-429.
- 327 Hack, J.T., 1982. Physiographic division and differential uplift in the piedmont and
328 Blue Ridge. U.S. Geological Survey Professional Paper 1265, 1-49.
- 329 Hare, P.W. & Gardner, T.W., 1985. Geomorphic indicators of vertical neotectonism
330 along converging plate margins. Nicoya Peninsula, Costa Rica. In: Morisawa, M. Hack
331 J.T. (Eds), *Tectonic Geomorphology. Proceedings of the 15th Annual Binghamton*
332 *Geomorphology Symposium*. Allen and Unwin, Boston, 123-134.
- 333 Karimi, A.R., 1999. Geological map of Kermanshah area, scale 1:100000, *Geologic*
334 *Survey of Iran*.
- 335 Keller, E.A., 1986. Investigation of active tectonics: use of surficial Earth processes.
336 In: Wallace RE. (Ed), *Active tectonics. Studies in Geophysics*, National Academy
337 press. Washington DC, 136-147.
- 338 Keller, EA. & Pinter, N., 2002. *Active tectonics: Earthquakes, Uplift, and Landscape*
339 (2nd Ed.). Prentice Hall, New Jersey, 432.
- 340 Memarian, H., 2001. *Geology for engineers*, Tehran University Press, (In Persian).
- 341 Mirzaei, N., Gao, M. & Chen, Y.T., 1998. seismic source regionalization for seismic
342 zoning of Iran: Major seismotectonic provinces, *Journal of Earthquake Prediction*
343 *Research*, 7, 465-495.
- 344 Molin, P., Pazzaglia, F.J. & Dramis, F., 2004. Geomorphic expression of active
345 tectonics in a rapidly-deforming forearc, sila massif. Calabria, southern Italy. *American*
346 *Journal of Science*, 304, 559-589.
- 347 Nazari, H., 1998. Geological map of Harsin area scale 1:100000 *Geologic Survey of*
348 *Iran*.

349 Ramirez-Herrera, M.T., 1998. Geomorphic assessment of active tectonics in the
350 Acambay Graben, Mexican volcanic belt. *Earth Surface Processes and Landforms* 23,
351 317-332.

352 Rockwell, T.K., Keller, E.A. & Jonson, D.L., 1985. Tectonic geomorphology of
353 alluvial fans and mountain fronts near Ventura, California. In: Morisawa, M. (Ed.),
354 *Tectonic Geomorphology. Proceedings of the 15th Annual Geomorphology*
355 *Symposium*. Allen and Unwin Publishers, Boston, 183-207.

356 Sadeghian, M. & Delavar, S.T., 2007. Geological map of Kamyaran area scale
357 1:100000 Geologic Survey of Iran.

358 Silva, P.G., 1994. *Evolution geodinamica de la depression del Guadalentín desde el*
359 *Mioceno superior hasta la actualidad: Neotectónica y geomorfología*, Ph.D. Dissertation,
360 Complutense University, Madrid.

361 Silva, P.G., Goy, J.L., Zazo, C. & Bardajm, T., 2003. Fault generated mountain fronts in
362 Southeast Spain: geomorphologic assessment of tectonic and earthquake activity.
363 *Geomorphology*, 250, 203-226.

364 Strahler, A.N., 1952. Hypsometric (area-altitude) analysis of erosional topography
365 *Geological Society of America Bulletin* 63, 1117-1142.

366 Wells, S.G., Bullard, T.F., Menges, T.M., Drake, P.G., Karas, P.A., Kelson, K.I., Ritter,
367 J.B. & Wesling, J.R., 1988. Regional variations in tectonic geomorphology along
368 segmented convergent plate boundary, Pacific coast of Costa Rica. *Geomorphology* 1,
369 239-265.

370
371

372 **Table 1: Values of 6 geomorphic indices for 88 subbasins of the Gharasu river basin**
373 **(Sl: stream length –gradient index; Af: drainage basin asymmetry; Hi: hypsometric**
374 **integral; Vf: ratio of valley floor width to valley height; Bs: index of drainage basin**
375 **shape; J: index of mountain-front sinuosity).**

376

Sub basin	Area	SI	Af	Bs	J	Vf	Hi
1	135.41	147.38	33.17	2.36	1.32 1.08 1.22 1.20 1.49	0.00 0.41	0.14
2	12.97	62.00	69.70	2.83	1.32	---	0.25
3	9.32	37.89	37.64	3.17	1.32	---	0.16
4	7.98	74.57	47.61	3.45	1.32	---	0.32
5	11.02	81.64	24.45	2.80	1.32	---	0.28
6	76.51	262.87	91.81	2.52	1.56 1.20 1.22	---	0.23
7	20.20	170.60	71.66	4.09	1.32	---	0.38
8	10.36	51.40	37.58	4.00	---	---	0.22
9	19.54	374.88	44.25	2.20	---	---	0.36
10	19.40	139.87	57.75	1.55	---	---	0.41
11	12.51	77.73	26.44	2.62	1.56	2.58	0.43
12	13.81	45.95	23.21	2.59	1.32	---	0.18
13	33.56	261.56	53.07	2.09	---	---	0.44
14	48.18	203.76	57.60	1.53	---	---	0.32
15	66.80	137.40	35.70	2.51	1.56 1.15 1.13	2.63 0.79 1.44 5.51 9.34 11.81	0.30
16	56.55	87.24	19.18	1.80	1.32	---	0.27
17	28.44	108.42	50.99	2.07	1.20	---	0.42
18	10.29	67.44	56.10	1.93	---	---	0.44
19	31.38	95.15	68.43	2.08	1.32	18.39	0.25
20	22.68	177.54	66.01	2.27	---	---	0.33
21	38.81	1362.04	39.78	1.63	1.32	---	0.36
22	25.60	189.27	70.26	2.61	---	---	0.35
23	16.40	231.04	85.06	2.18	1.32	9.41	0.32
24	25.76	103.17	37.29	2.11	---	---	0.49
25	11.33	39.58	46.26	1.68	---	---	0.47
26	13.87	3	46.04	1.50	---	---	0.34
27	14.46	50.84	51.13	2.04	---	---	0.45
28	12.27	175.01	64.18	4.90	1.32	1.53 7.14	0.24
29	21.62	137.13	54.33	2.53	1.32	---	0.16
30	22.50	119.81	26.60	2.80	---	---	0.31
31	10.81	161.70	57.75	6.57	---	---	0.34
32	91.41	171.37	71.06	0.93	1.49 1.27 1.13	3.26 4.82	0.39
33	103.42	170.66	65.71	1.16	---	---	0.24
34	157.15	106.04	39.47	1.95	1.49 1.28 1.16 1.20	---	0.23
35	51.83	43.76	44.92	2.03	1.47	---	0.11
36	15.31	30.80	62.75	2.56	1.47	---	0.10
37	21.79	47.91	63.53	2.05	---	---	0.21
38	47.53	254.04	60.69	2.20	1.47	1.44	0.17
39	51.89	54.58	65.76	1.52	---	---	0.25
40	20.21	20.90	29.02	2.08	1.51	---	0.23

41	21.29	13.55	62.40	1.21	1.28	---	0.17
42	15.00	89.76	47.07	0.98	1.47	1.56 0.18	0.17
43	16.98	67.68	31.48	1.58	1.47	---	0.25
44	100.39	137.96	25.03	2.26	1.51	---	0.17
45	72.40	30.64	83.18	1.36	---	---	0.14
46	35.74	116.66	47.17	3.12	1.51	1.05	0.29
47	105.46	79.98	15.13	2.70	1.49 1.27	---	0.21
48	21.91	102.71	66.03	2.98	1.27	4.14	0.21
49	9.01	--	64.77	1.62	---	---	0.24
50	155.18	154.77	44.84	1.14	1.47	0.40	0.27
51	53.96	26.48	70.40	2.15	1.28 1.27	---	0.14
52	42.75	9.65	46.92	1.23	1.27	12.41	0.11
53	108.39	125.42	45.95	4.61	1.51	---	0.13
54	38.29	85.19	48.13	6.11	1.43	3	0.22
55	47.24	132.10	59.68	2.47	1.43	---	0.15
56	194.59	558.88	58.04	0.70	2.00	0.08	0.18
57	18.32	---	16.59	2.73	1.45	---	0.07
58	146.18	112.99	69.69	3.81	1.51	0.38	0.28
59	107.98	101.77	59.69	2.46	1.45 1.24 1.30	0.2 0.2 0.85	0.09
60	38.55	1289.77	59.04	3.05	2.00	0.38 0.50	0.40
61	24.70	94.38	61.94	1.69	1.45 1.30 1.14	0.82	0.23
62	24.43	39.60	52.66	1.31	2.00	---	0.15
63	12.32	965.73	60.08	2.31	1.42	---	0.53
64	18.38	9.82	50.90	1.70	1.45	---	0.27
65	7.28	27.89	13.89	1.43	2.00	---	0.22
66	118.71	76.09	66.94	1.55	1.26 1.25	13.51 9.66 19.44	0.17
67	152.17	85.69	61.84	0.74	1.23 1.42 1.21	4.89 3.10 3.32 1.59	0.20
68	53.01	403.87	64.82	2.78	1.14	---	0.33
69	11.70	197.91	48.41	2.55	1.59	1.38	0.41
70	28.94	742.88	33.88	5.36	1.42	---	0.49
71	24.79	10.93	43.62	3.22	1.59	---	0.44
72	98.37	137.32	57.94	1.77	1.25	---	0.36
73	14.85	69.15	70.96	3.42	---	---	0.36
74	20.40	129.56	62.15	2.74	1.23 1.68	---	0.31
75	22.75	212.17	63.63	2.27	1.59	1.97	0.42
76	12.66	98.62	58.45	2.45	1.68	---	0.31
77	81.52	194.22	63.26	1.40	1.23	---	0.35
78	58.74	96.92	77.88	1.45	---	---	0.32
79	12.90	79.93	39.70	3.43	1.68	---	0.29
80	16.45	35.93	18.43	1.92	1.68	---	0.24
81	111.95	43.00	54.81	1.36	---	---	0.25
82	49.20	224.02	69.93	1.79	1.59	1.91 0.62	0.42
83	1048.63	60.79	49.80	---	1.16 1.16	1.07 1.35	0.13

						1.45	2.55		
						1.14	12.01		
						1.32	4.26		
						1.32	1.79		
						1.56			
						1.20			
						1.28			
						1.34			
						1.14			
						1.23			
						1.59			
						1.51			
						1.47			
						2.00			
						1.68			
						1.42			
84	74.01	270.20	39.53	1.38	1.28	---	---	0.15	
85	160.89	301.99	30.90	1.32	2.04	1.45	0.38		
						1.74			
						0.79			
86	42.34	91.71	53.13	2.96	---	---	---	0.21	
87	53.25	144.37	38.13	1.17	---	---	---	0.43	
88	177.04	1669.67	43.45	2.01	1.34	0.28	0.40		
						0.08			
						0.85			
						1.48			
89	167.97	73.37	61.94	1.05	---	---	---	0.26	

377
378
379

380 **Table 2:** Classification of the Iat (relative tectonic activity index) in the subbasins of the
381 Gharasu river basin (Sl: stream length –gradient index; Af: drainage basin asymmetry;
382 Hi: hypsometric integral; Vf: ratio of valley floor width to valley height;Bs: index of
383 drainage basin shape; J: index of mountain-front sinuosity).

Sub basin	Area	Sl	Af	Bs	J	Vf	Hi	S/n	Iat
1	135.41	3	1	3	2	1	1	1.83	2
2	12.97	3	1	3	2	---	3	2.40	3
3	9.32	3	2	2	2	---	3	2.40	3
4	7.98	3	3	2	2	---	3	2.60	4
5	11.02	3	1	3	2	---	3	2.40	3
6	76.51	3	1	3	2	---	3	2.40	3
7	20.20	3	1	1	2	---	3	2.00	3
8	10.36	3	2	2	---	---	3	2.50	4
9	19.54	2	3	3	---	---	3	2.75	4
10	19.40	3	2	3	---	---	2	2.50	4
11	12.51	3	1	3	3	3	2	2.50	4
12	13.81	3	1	3	2	---	3	2.40	3
13	33.56	3	3	3	---	---	2	2.75	4
14	48.18	3	2	3	---	---	3	2.75	4
15	66.80	3	2	3	2	3	3	2.67	4
16	56.55	3	1	3	2	---	3	2.40	3
17	28.44	3	3	3	2	---	2	2.60	4

18	10.29	3	3	3	---	---	2	2.75	4
19	31.38	3	1	3	2	3	3	2.50	4
20	22.68	3	1	3	---	---	3	2.50	4
21	38.81	1	2	3	2	---	3	2.50	4
22	25.60	3	1	3	---	---	3	2.50	4
23	16.40	3	1	3	2	3	3	2.75	4
24	25.76	3	2	3	---	---	2	3.00	4
25	11.33	3	3	3	---	---	2	2.75	4
26	13.87	3	3	3	---	---	3	2.33	3
27	14.46	3	3	3	---	---	2	2.80	4
28	12.27	3	2	1	2	3	3	2.50	4
29	21.62	3	3	3	2	---	3	2.25	3
30	22.50	3	1	3	---	---	3	2.50	4
31	10.81	3	2	1	---	---	3	2.50	4
32	91.41	3	1	3	2	3	3	2.60	4
33	103.42	3	1	3	---	---	3	2.80	4
34	157.15	3	2	3	2	---	3	2.60	4
35	51.83	3	3	3	2	---	3	2.75	4
36	15.31	3	2	3	2	---	3	2.67	4
37	21.79	3	2	3	---	---	3	2.50	4
38	47.53	3	2	3	2	3	3	2.60	4
39	51.89	3	1	3	---	---	3	2.60	4
40	20.21	3	1	3	3	---	3	2.67	4
41	21.29	3	2	3	2	---	3	2.40	3
42	15.00	3	3	3	2	2	3	2.60	4
43	16.98	3	1	3	2	---	3	2.50	4
44	100.39	3	1	3	3	---	3	3.00	4
45	72.40	3	1	3	---	---	3	2.40	3
46	35.74	3	3	3	3	3	3	2.50	4
47	105.46	3	1	3	2	---	3	2.67	4
48	21.91	3	1	3	2	3	3	2.50	4
49	9.01	---	2	3	---	---	3	2.40	3
50	155.18	3	3	3	2	1	3	2.83	4
51	53.96	3	1	3	2	---	3	2.60	4
52	42.75	3	3	3	2	3	3	2.50	4
53	108.39	3	3	1	3	---	3	2.60	4
54	38.29	3	3	1	2	3	3	2.17	3
55	47.24	3	2	3	2	---	3	2.25	3
56	194.59	1	2	3	3	1	3	2.17	3
57	18.32	---	1	3	2	---	3	2.33	3
58	146.18	3	1	2	3	1	3	1.83	2
59	107.98	3	2	3	2	1	3	2.50	4
60	38.55	1	2	2	3	1	2	3.00	4
61	24.70	3	2	3	2	2	3	2.20	3
62	24.43	3	3	3	3	---	3	2.80	4
63	12.32	3	2	3	2	---	1	2.60	4
64	18.38	3	3	3	2	---	3	2.50	4
65	7.28	3	1	3	3	---	3	2.67	4
66	118.71	3	1	3	2	3	3	2.40	3
67	152.17	3	2	3	2	3	3	2.83	4
68	53.01	2	2	3	2	---	3	1.40	1
69	11.70	3	3	3	3	3	2	2.50	4

70	28.94	1	1	1	2	---	2	2.60	4
71	24.79	3	3	2	---	---	2	2.25	3
72	98.37	3	2	3	2	---	3	2.80	4
73	14.85	3	1	2	---	---	3	2.67	4
74	20.40	3	2	3	3	---	3	2.80	4
75	22.75	3	2	3	3	3	2	2.60	4
76	12.66	3	2	3	3	---	3	2.50	4
77	81.52	3	2	3	2	---	3	2.60	4
78	58.74	3	1	3	---	---	3	2.60	4
79	12.90	3	2	2	3	---	3	3.00	4
80	16.45	3	1	3	3	---	3	2.50	4
81	111.95	3	3	3	---	---	3	2.80	4
82	49.20	3	1	3	3	3	2	2.83	4
83	1048.63	3	3	---	2	3	3	2.50	4
84	74.01	3	3	3	2	---	3	2.75	4
85	160.89	3	2	3	3	3	3	2.00	3
86	42.34	3	1	3	---	---	3	3.00	4
87	53.25	3	3	3	---	---	2	2.80	4
88	177.04	1	2	3	2	2	2	2.50	4
89	167.97	3	3	3	---	---	3	2.20	3

384

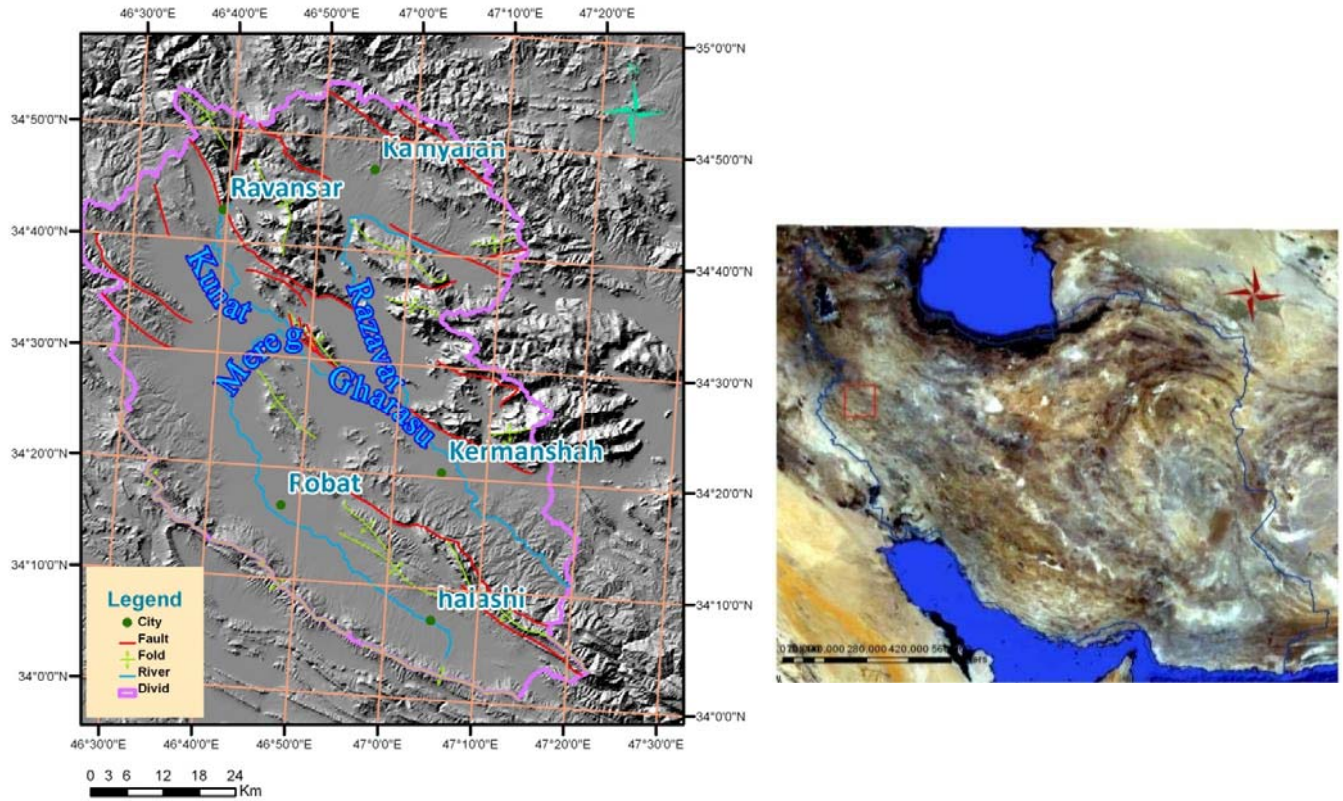
385

386

387

388 **Table 3:** The area and occupation percentage of each class of geomorphic indices.

geomorphic indices	Not value		Class1		Class2		Class3	
	area	occupation percent	area	occupation percent	area	occupation percent	area	occupation percent
Vf	2495.17	45.78	777.88	13.96	216.73	3.8	1981.05	36.2
Smf	1020.72	19.32	----	----	3454.9	63.01	995.22	17.86
Bs	1048.62	19.96	218.89	3.92	264.92	4.8	3938.40	70.69
Af	----	----	1596.60	28.65	1730.88	31.6	2143.36	38.47
Sl	27.32	0.69	477.93	8.57	72.54	1.70	4893.04	87.83
Hi	----	----	147.73	2.65	561.95	10.87	4761.16	85.66



389 **Figure 1.** Location of the study area in Iran and Zagros fold-thrust belt.

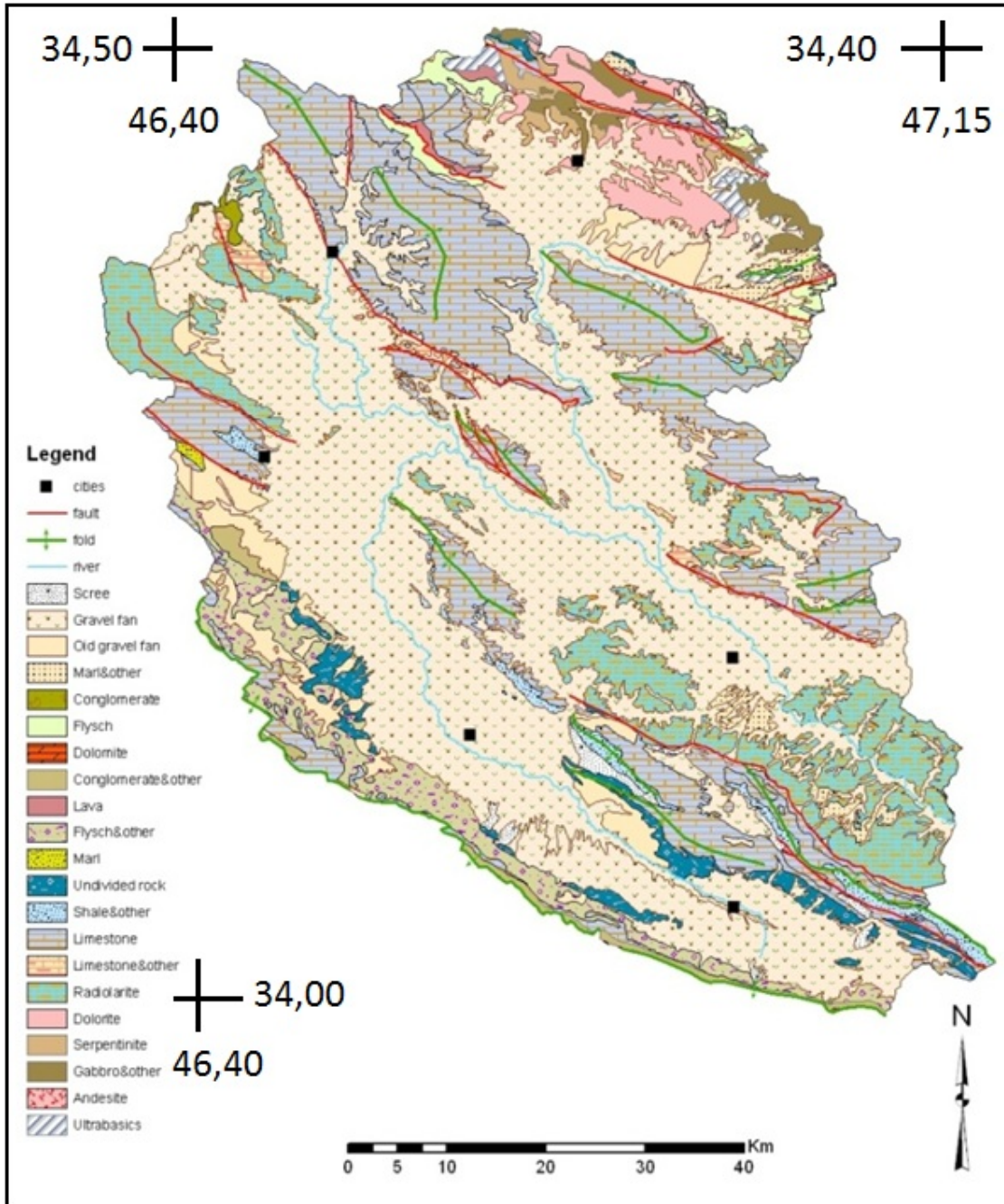
390

391

392

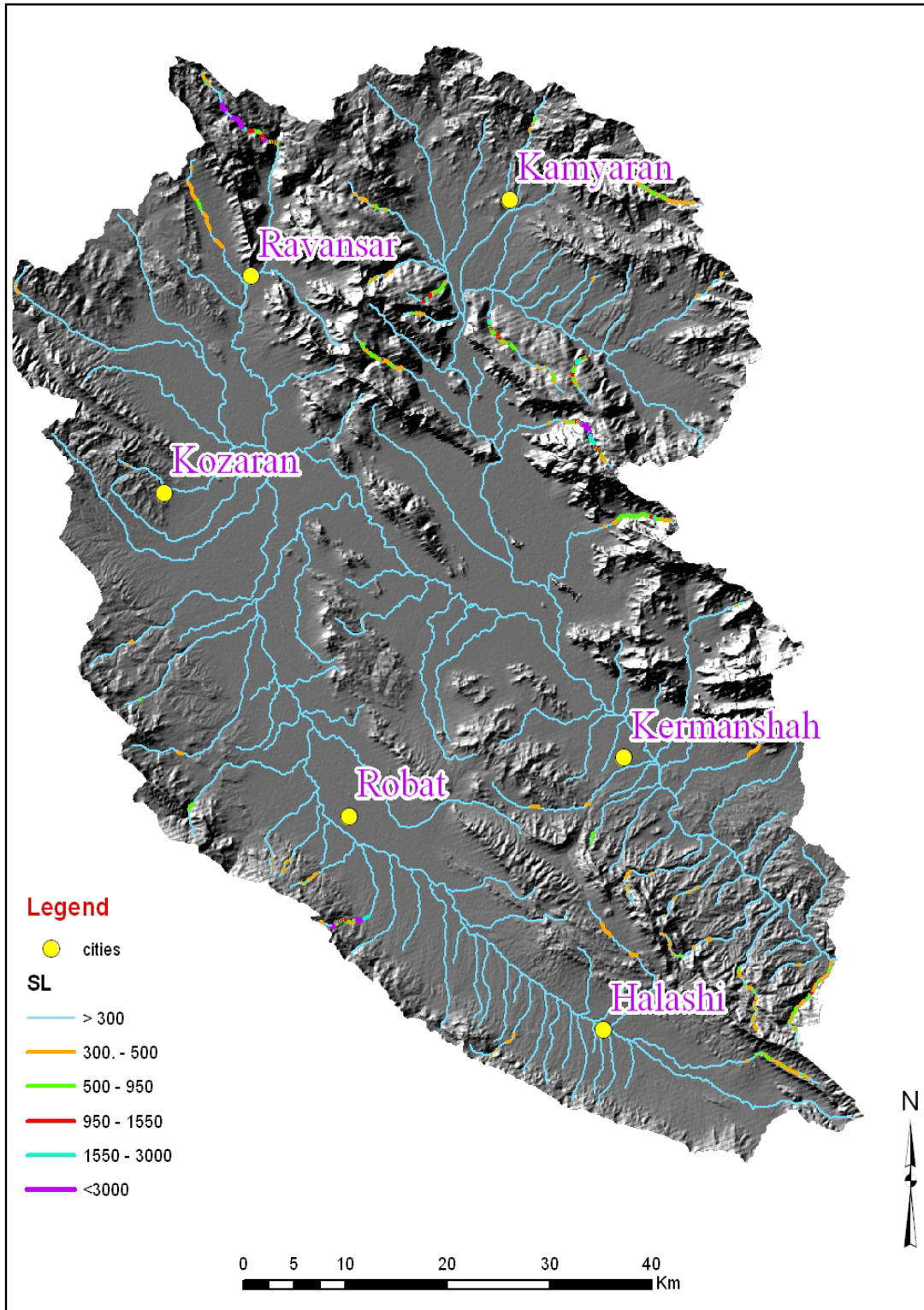
393

394



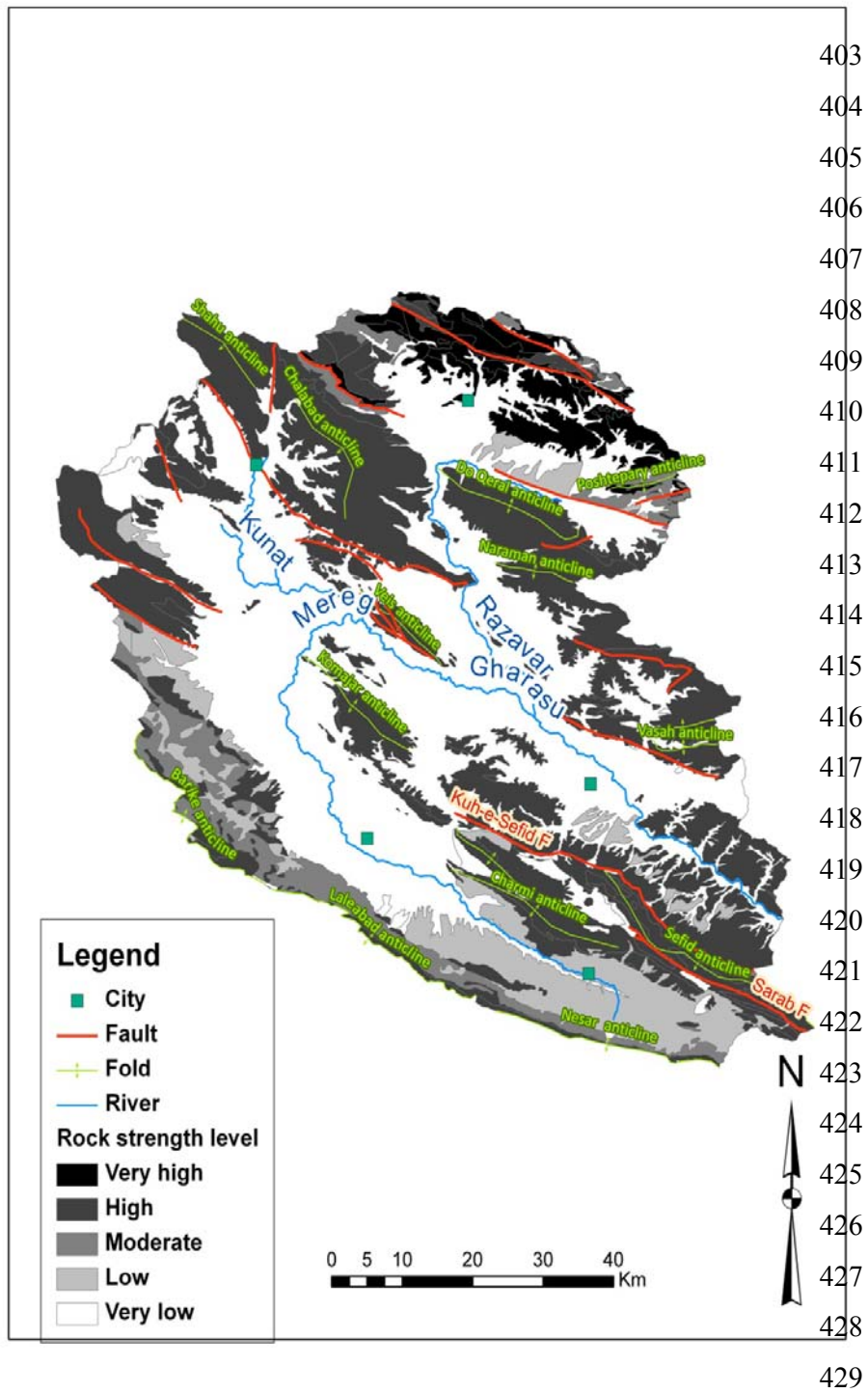
395
 396
 397
 398

Figure 2. Geological map(1:250000) in the study area.



399
 400
 401
 402

Figure 3. SL index along the drainage network.



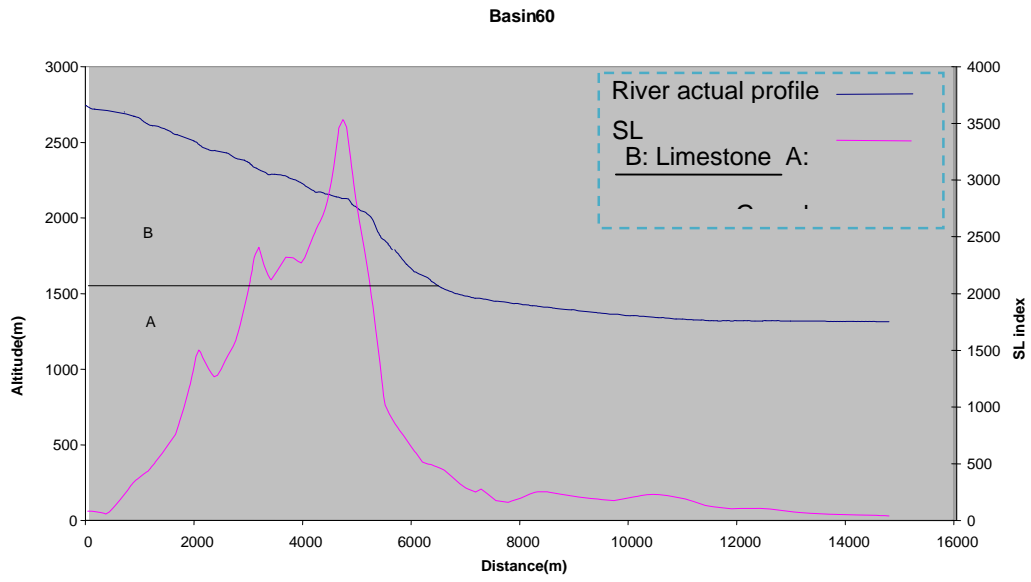
430

431 **Figure 4.**Distribution of rock strength levels in the area.

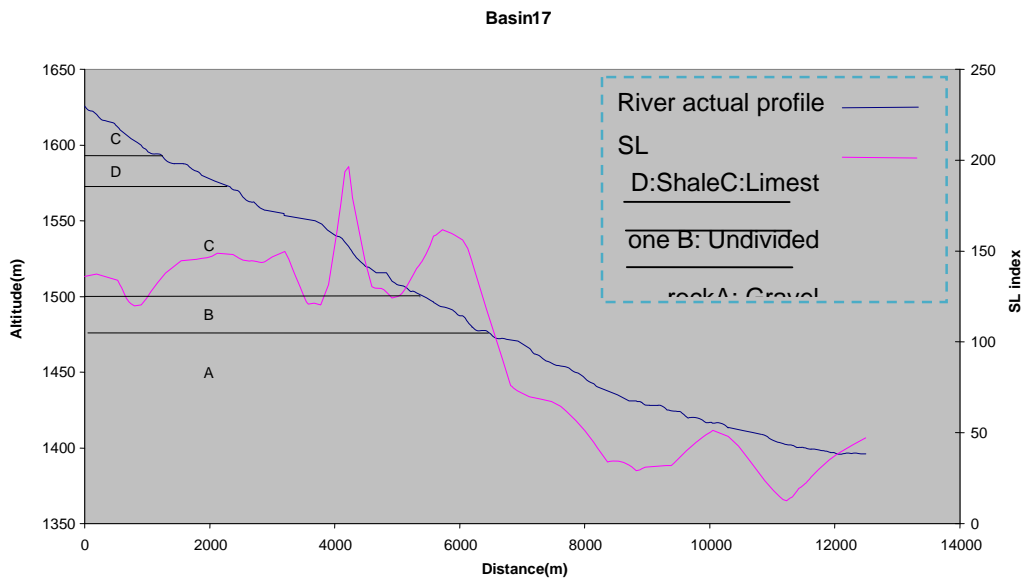
432

433

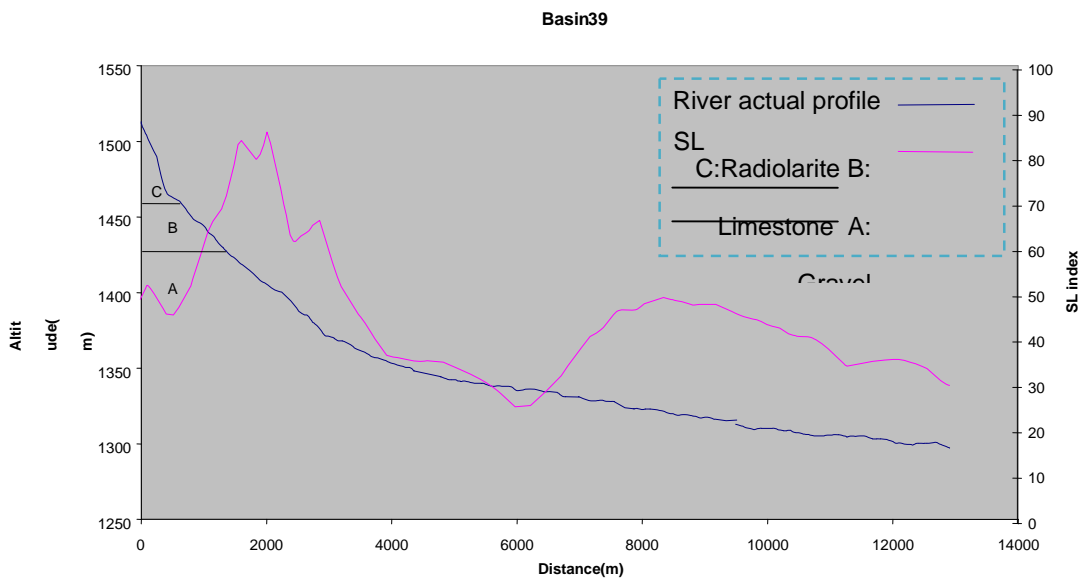
434
435



436



437



438

439

440

441

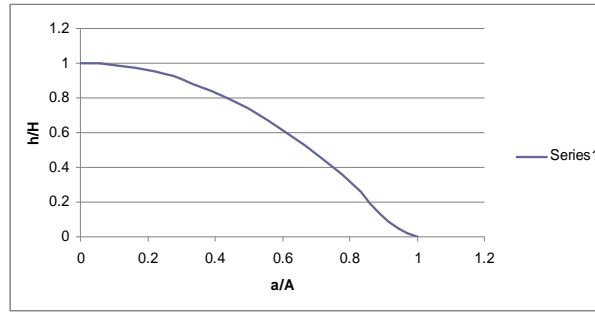
442

443 **Figure 5 .** Longitudinal river profiles and measured SL values for three subbasins in the

444 study area.

445

446

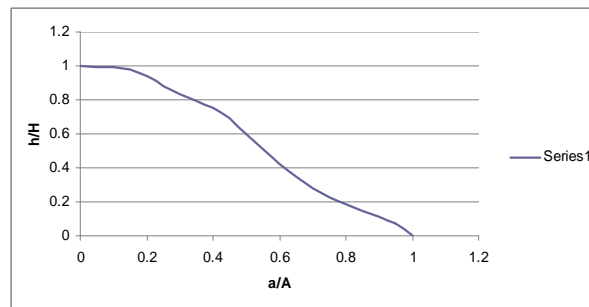


447

Subbasin 22

448

449



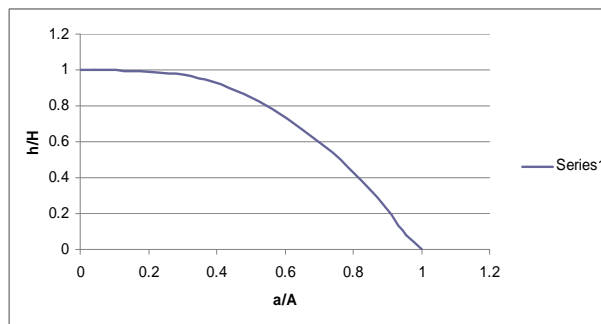
450

Subbasin 82

451

452

453



454

Subbasin 89

455

456

457

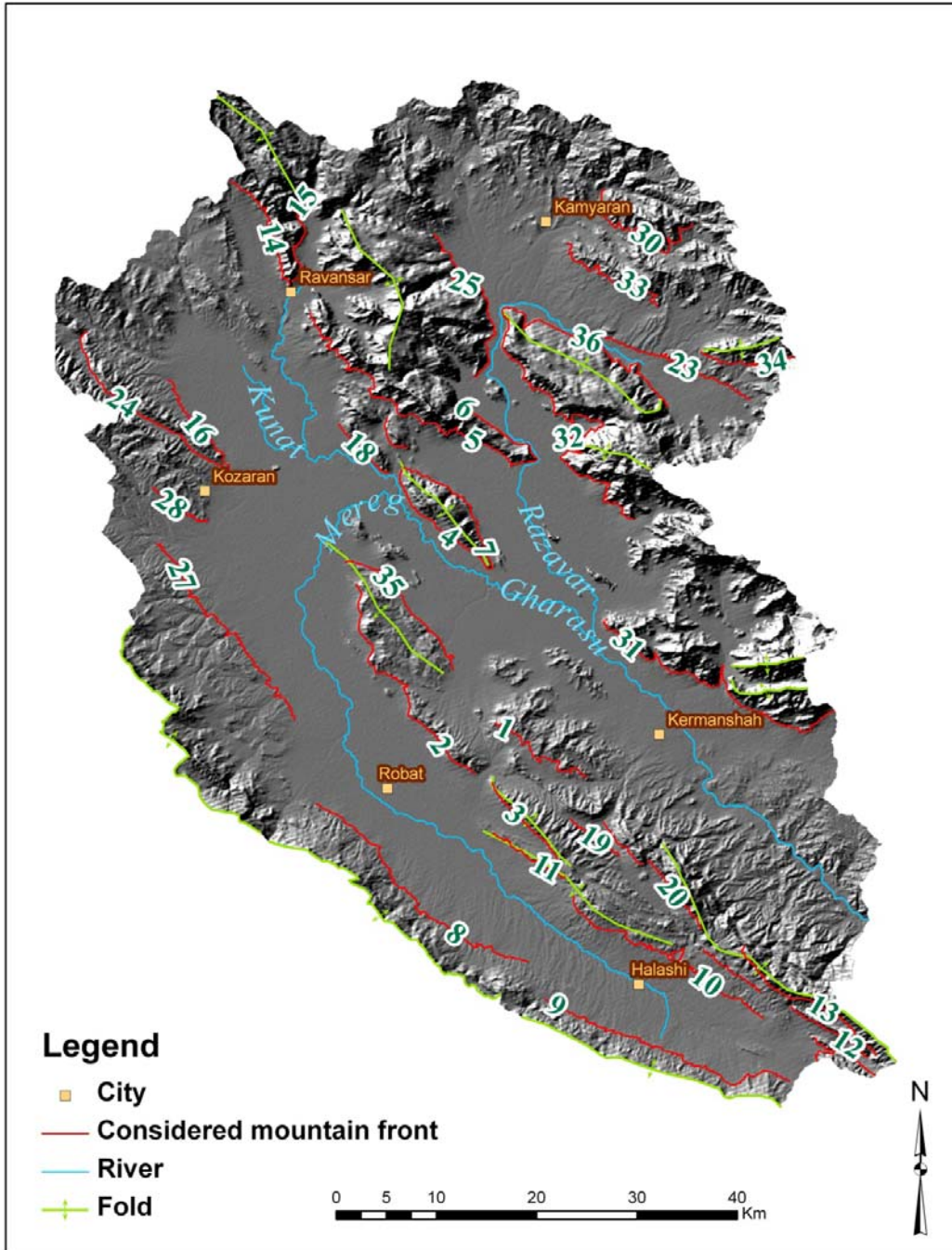
458 **Figure 6.**Hypsometry- curves of 3 subbasins in the study area. (A) is the total surface of

459 the basin. (a) is the surface area within the basin above a given line of elevation(h). (H)

460 is the highest elevation of the basin.

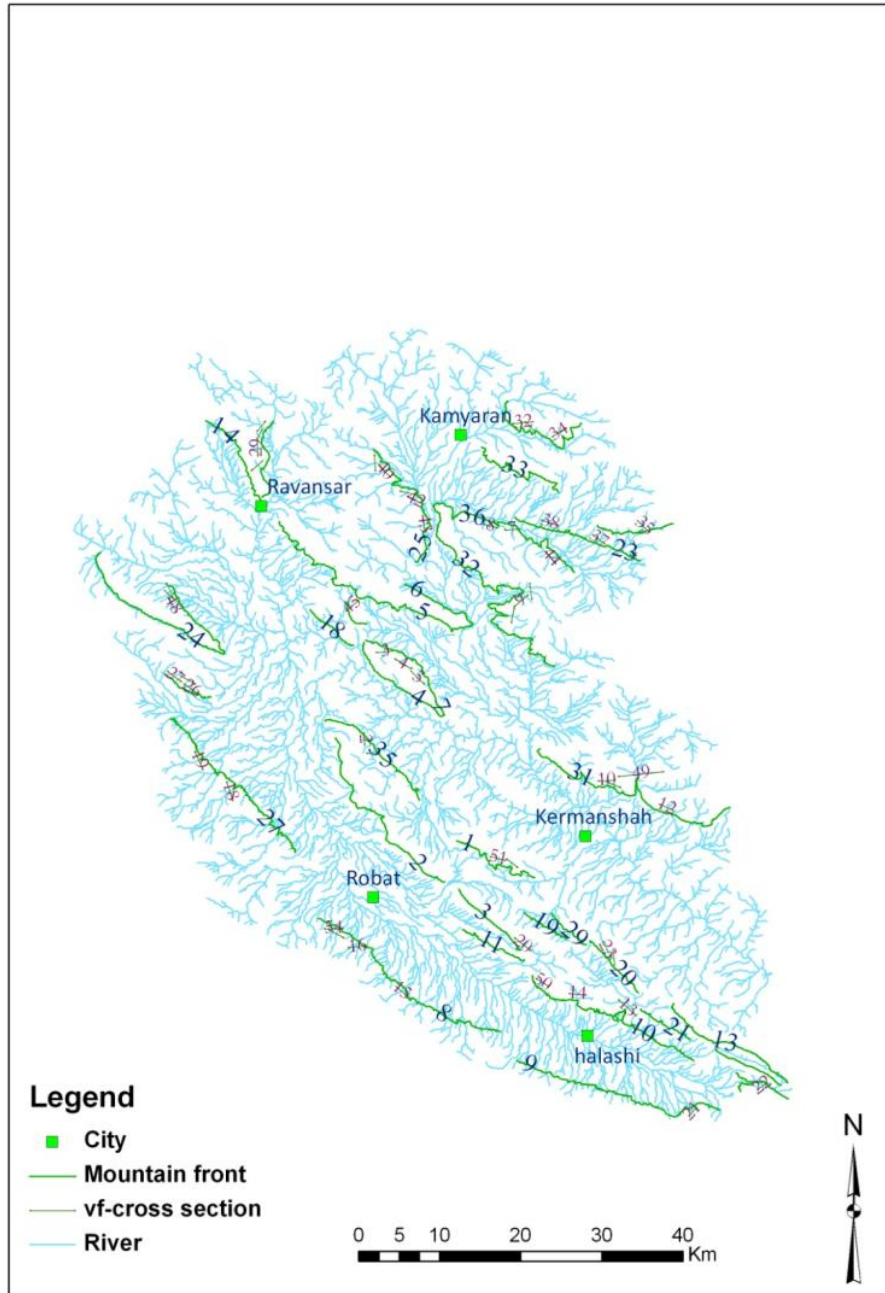
461

462
463



464
465

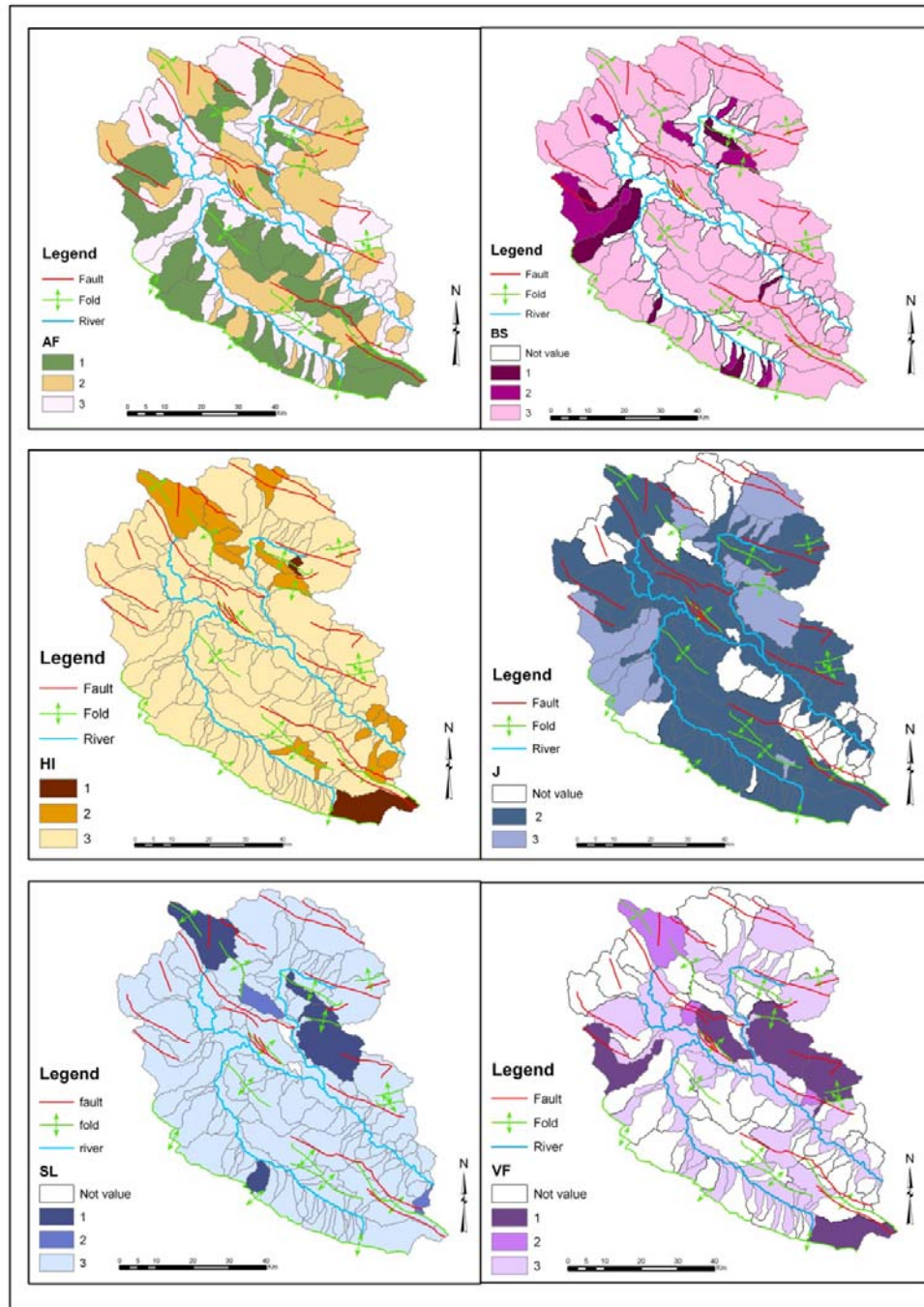
Figure7 .Thirty-six Mountain fronts for the assessment of the J index.



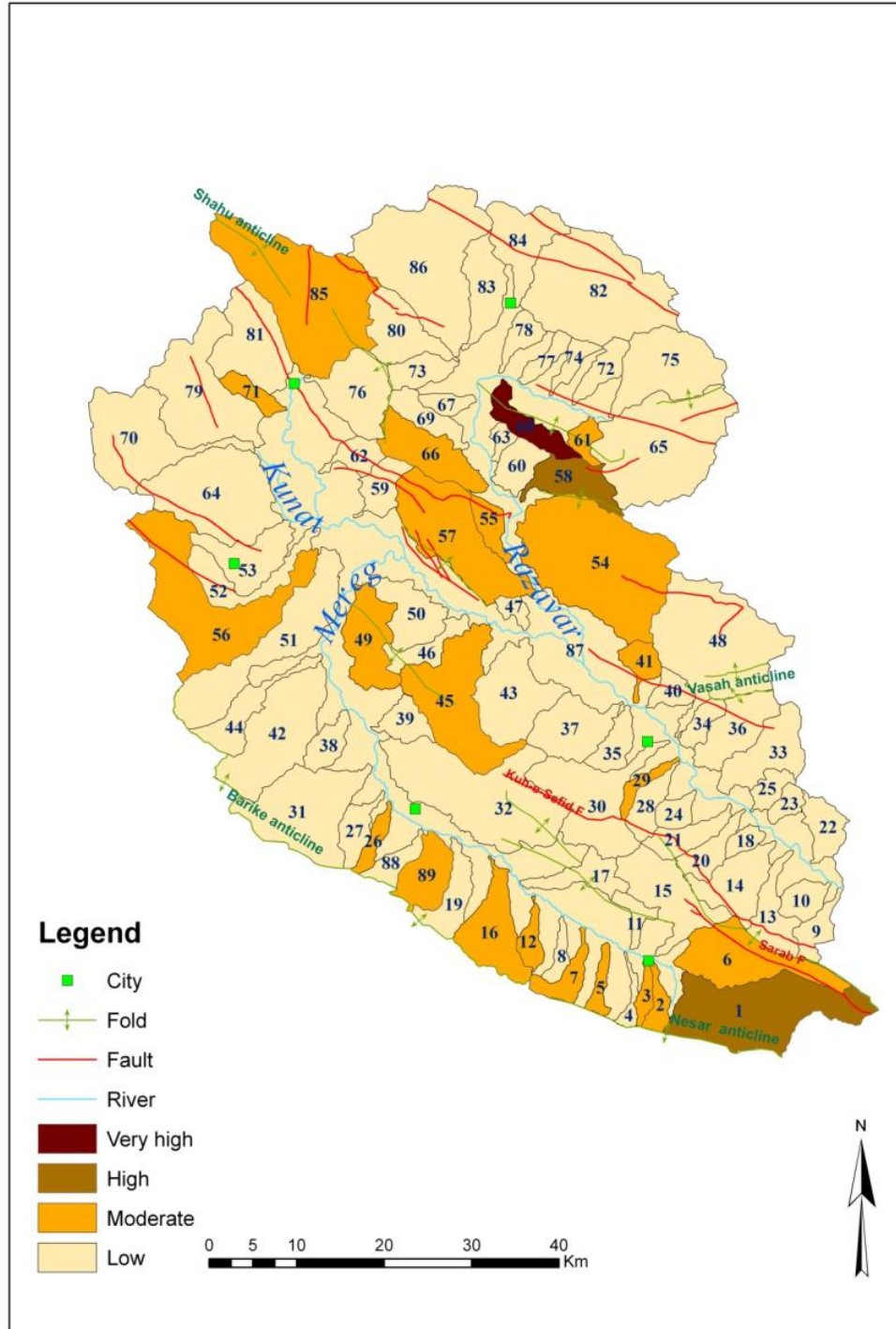
466
467

468 **Figure8** .Location of section for V fcalculation.

469



470
 471 **Figure9** .Distribution of 6 indices Hi, Vf, J, Bs, Af, SL and classification of them to 3
 472 classes.
 473



474
 475
 476
 477

Figure10.Distribution of Iat classes.

478
479
480
481



482
483

484

485 **Figure 11.**A view of faulting at north of the study area, looking to north western.

486
487
488
489
490
491
492
493
494
495
496
497
498
499
500



501
502
503

504

505 **Figure12** .Intense folding and crushing in Biseton limestone placed on 60km northeast
506 of the village Bencheleh, looking to northeastern.

507
508
509
510
511
512
513
514



515
516
517
518

519 **Figure 13.** A view of the Kuh-e Sefid Fault placed on 6km east of Halashi, looking to
520 north.

521
522
523
524
525
526
527
528
529
530
531
532
533
534